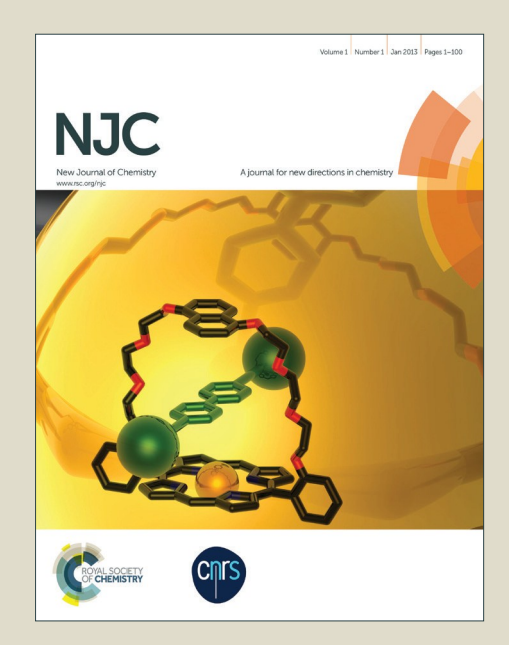
NJC

Accepted Manuscript



This is an *Accepted Manuscript*, which has been through the Royal Society of Chemistry peer review process and has been accepted for publication.

Accepted Manuscripts are published online shortly after acceptance, before technical editing, formatting and proof reading. Using this free service, authors can make their results available to the community, in citable form, before we publish the edited article. We will replace this Accepted Manuscript with the edited and formatted Advance Article as soon as it is available.

You can find more information about *Accepted Manuscripts* in the **Information for Authors**.

Please note that technical editing may introduce minor changes to the text and/or graphics, which may alter content. The journal's standard <u>Terms & Conditions</u> and the <u>Ethical guidelines</u> still apply. In no event shall the Royal Society of Chemistry be held responsible for any errors or omissions in this *Accepted Manuscript* or any consequences arising from the use of any information it contains.



Syntheses and luminescence of $La_{1-x}Eu_x[B_8O_{11}(OH)_5]$ and β -

$$La_{1-x}Eu_xB_5O_9 \ (0 \le x \le 0.135)$$

Xiaorui Sun,^a Wenliang Gao,^a Rihong Cong,^{a*} Tao Yang^{a*}

^a College of Chemistry and Chemical Engineering, Chongqing University, Chongqing 400044, P. R. China

^{*}Correspondence authors, email: congrihong@cqu.edu.cn, taoyang@cqu.edu.cn; Tel: +86-23-65105065.

Abstract

Luminescence study on rare earth borates have been active for a long time. Here we performed a careful synthesis to prepare pure samples of La_{1-x}Eu_x[B₈O₁₁(OH)₅] ($0 \le x \le 0.135$) by boric acid flux method, and after evaluating its thermal behavior by thermogravimetric analysis and powder X-ray diffraction, an appropriate thermal treatment was applied to prepare anhydrous β-La_{1-x}Eu_xB₅O₉ (810 °C, 10 h), thus allowing the study on their Eu³⁺-luminescence in a relatively wide range of Eu³⁺-concentration. The comparatively strong f-f transition of La_{1-x}Eu_x[B₈O₁₁(OH)₅] in the excitation spectra suggests its potential as red-emitting phosphors for white-light emitting diodes, which can be efficiently excited by ultraviolet-light emitting diode chips and show the strongest red emission at 622 nm. On the contrary, β-La_{1-x}Eu_xB₅O₉ show a very intense O²⁻ \rightarrow Eu³⁺ CT absorption, and give strong red emissions with red/orange ratios ~2.4. Both the La_{1-x}Eu_x[B₈O₁₁(OH)₅] and β-La_{1-x}Eu_xB₅O₉ show no concentration quenching up to the maximal x = 0.135, which is as-expected due to their large spatial distances between rare earth cations. It is the first time to study the luminescent performance when La[B₈O₁₁(OH)₅] and β-LaB₅O₉ were used as the hosts. In addition, La_{0.93}Eu_{0.07}[B₈O₁₁(OH)₅] was selected as a representative to study the luminescence evolution during thermal treatments.

Keywords: Rare earth borates, boric acid flux method, luminescence, thermal decomposition.

Introduction

Luminescent materials doped with trivalent lanthanide ions (Ln^{3+}) possess high quantum yields, sharp emission lines, long lifetimes and superior photo-stabilities, which therefore have great potentials in chromatic displays, solid-state lasers and so on. 1-4 Rare earth borates are well known good hosts for doping Ln^{3+} activators, and show high transparency, good thermal stability, exceptional optical damage threshold, and high luminescence efficiency.⁵⁻⁷ The problem is that only three rare earth borates existed in the Ln_2O_3 -B₂O₃ phase diagrams if prepared by high temperature solid state reactions, including oxyborate, 8,9 orthoborate 10 and metaborate. 11,12 To solve this problem, people developed several new synthetic methods in the past decades, including high-pressure/high-temperature technique, ^{13,14} sol-gel process, 15 hydrothermal 16 and boric acid flux methods. 17,18 Among them, hydrothermal and boric acid flux methods are particularly effective for obtaining novel hydrous borates. For examples, $Ln[B_5O_8(OH)]NO_3 \cdot 3H_2O(Ln = La, Ce), Ln[B_6O_9(OH)_3](Ln = Sm-Lu), Ln[B_8O_{11}(OH)_5](Ln = La-Nd),$ and $Ln[B_9O_{13}(OH)_4] \cdot H_2O$ (Ln = Pr-Er) were prepared by boric acid flux method. 17,18 It allows the following investigations on luminescence of those new polyborates. For example, systematic luminescence investigations revealed that $Sm_{1-x}Eu_x[B_9O_{13}(OH)_4] \bullet H_2O$ and $Gd_{1-x}Eu_x[B_6O_9(OH)_3]$ ($0 \le x$ \leq 1) both exhibited strong Eu³⁺ f-f absorptions, suggesting their potential applications as near UV-LED chips. 19,20

On the other hand, the calcination of hydrous polyborates usually leads to the formation of new polyborates other than three already-reported anhydrous rare earth borates. $^{17-20}$ Indeed, the previous studies proved that α - Ln_{1-x} EuB₅O₉ (Ln = Sm or Gd) were excellent phosphors, which are the anhydrous products of Sm_{1-x}Eu_x[B₉O₁₃(OH)₄]•H₂O and Gd_{1-x}Eu_x[B₆O₉(OH)₃], respectively. 19,20 All these new rare earth polyborates possess large polyborate ions and thus provide large spatial separation for Eu³⁺ activators, which is advantageous to avoid the concentration quenching problem. Indeed, none of above mentioned polyborates show any concentration quenching.

As α - LnB_5O_9 (Ln = Sm or Gd) was proved to be an outstanding phosphor host, thus we are motivated to study the performance of another pentaborate with larger rare earth cations, i.e. β -LaB₅O₉.

Though with the same Ln/B ratio in the formula, α - and β - LnB_5O_9 possess different types of structure (For more structural details, please refer to references 17 and 18). In fact, a very rough experiment has been performed in literature about the luminescence of Eu³⁺ doped β-LaB₅O₉. ¹⁸ The dominant emission was the ${}^5D_0 \rightarrow {}^7F_2$ transition, however, it was reported that the optimal Eu³⁺-concentration is around 0.6 atom%, which is a little suspicious according to our recent analyses and the study on α - LnB_5O_9 (Ln = Sm or Gd). ^{15,19} As shown in Fig. 1, from the structural aspect, the nearest La-La distance in β -LaB₅O₉ is 4.45 Å, which is even longer than the Sm-Sm distance in α -SmB₅O₉ (3.78 Å). Base on the absence of concentration quenching in the complete solid solutions of α -Sm_{1-x}Eu_xB₅O₉ (0 < x ≤ 1), ¹⁹ a very low quenching concentration (x = 0.006) for β -La_{1-x}Eu_xB₅O₉ reported in literature is unreasonable and needs to be re-studied. In addition, the synthesis of β -La_{1-x}Eu_xB₅O₉ is relatively difficult than that of α -Sm_{1-x}Eu_xB₅O₉, because of the size mismatch between La³⁺ and Eu³⁺.

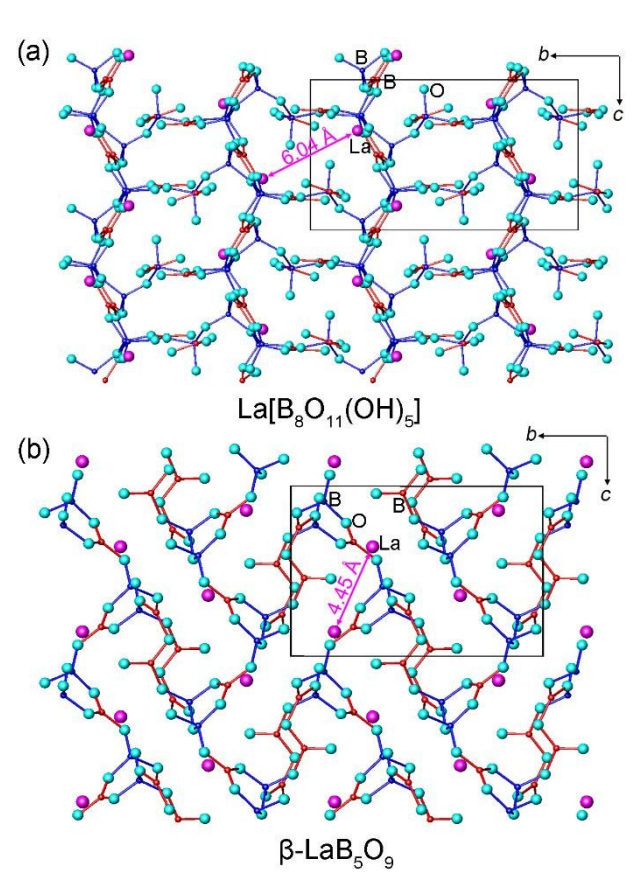


Fig. 1 Representative structural views of La[$B_8O_{11}(OH)_5$] and β -LaB $_5O_9$. The nearest La-La distances were highlighted as 6.04 and 4.45 Å, respectively.

In this work, a partial solid solutions of $La_{1-x}Eu_x[B_8O_{11}(OH)_5]$ ($0 \le x \le 0.135$) were prepared for the first time by boric acid flux method. Attentions need to be paid to avoid the formation of other rare earth polyborate impurities. Thereafter, it allowed us to perform the calcinations on hydrous borates, and highly crystalline anhydrous β -La_{1-x}Eu_xB₅O₉ ($0 \le x \le 0.135$) was successfully obtained. We performed a systemic luminescence study in a relatively wide range of Eu^{3+} concentration, comparing to the work in literature (1 atom%).¹⁸ The red emissions for $La_{1-x}Eu_x[B_8O_{11}(OH)_5]$ were relatively weak probably due to abundant hydroxyl groups, and the absence of concentration quenching up to 13.5 atom% was realized experimentally. β -LaB₅O₉ is a good phosphor host for Eu^{3+} -doping with intense red emissions and shows no concentration quenching due to the large La-La distance. In addition, $La_{0.93}Eu_{0.07}[B_8O_{11}(OH)_5]$ was selected as a representative to study the luminescence evolution during thermal treatments.

Experimental

The syntheses of La_{1-x}Eu_x[B₈O₁₁(OH)₅] were carried out in closed Teflon autoclaves using boric acid flux method. Typically, 0.3 mmol of La₂O₃ and 24 mmol of H₃BO₃ (La/B = 1/40) were first mixed and ground thoroughly in an agate mortar, and were transferred into a 25 ml Teflon autoclave, then 0.5 mL of deionized water was added. The autoclave was sealed in a stainless-steel shell and heated at 240 $^{\circ}$ C in an oven for 5 days. The solid products were washed with water until the excess boric acid was completely removed. The resultant powder was white and was dried at 60 $^{\circ}$ C for further characterizations. By the same procedure, a series of Eu³⁺-doped samples La_{1-x}Eu_x[B₈O₁₁(OH)₅] (0.010 $^{\circ}$ C $^{\circ}$

Polycrystalline samples of β -La_{1-x}Eu_xB₅O₉ ($0 \le x \le 0.135$) were obtained by heating the as-synthesized La_{1-x}Eu_x[B₈O₁₁(OH)₅] ($0 \le x \le 0.135$) powder at 810 °C for 10 hours.

Table 1 Experimental mole ratios by ICP-AES method for selected samples.

Expected formula	Experimental mole ratio
	(La : Eu : B)
$La_{0.96}Eu_{0.04}[B_8O_{11}(OH)_5]$	0.945 : 0.055 : 7.98
La _{0.93} Eu _{0.07} [B ₈ O ₁₁ (OH) ₅]	0.925 : 0.075 : 7.96
La _{0.90} Eu _{0.10} [B ₈ O ₁₁ (OH) ₅]	0.899 : 0.101 : 7.77
La _{0.865} Eu _{0.135} [B ₈ O ₁₁ (OH) ₅]	0.854 : 0.146 : 8.02
β-La _{0.96} Eu _{0.04} B ₅ O ₉	0.946 : 0.054 : 5.12
β-La _{0.93} Eu _{0.07} B ₅ O ₉	0.922 : 0.078 : 5.15
β-La _{0.90} Eu _{0.10} B ₅ O ₉	0.881 : 0.119 : 5.05
β-La _{0.865} Eu _{0.135} B ₅ O ₉	0.859 : 0.141 : 5.68

Powder XRD data were collected at room temperature on a PANalytical X'pert diffractometer equipped with a PIXcel 1D detector (Cu Kα radiation). The operation voltage and current are 40 kV and 40 mA, respectively. Le Bail refinements were performed to obtain the cell parameters using TOPAS software package.²¹ Combined thermogravimetric analysis and differential scanning calorimeter (TG-DSC) analysis was performed on a Mettler-Toledo TGA/DSC1 instrument under N₂ flow. Photoluminescent spectra were measured on a Hitachi F4600 fluorescence spectrometer. The voltage of Xe lamp is fixed to be 700 V, and both of the input and output slits were selected to be 2.5 nm. The emission intensities are calculated from the integral of corresponding peaks.

Results and Discussion

Optimizing the synthetic conditions

As reported in literature, three different polyborates can be formed by boric acid flux method, including $Ln[B_6O_9(OH)_3]$, $Ln[B_9O_{13}(OH)_4] \cdot H_2O$ and $Ln[B_8O_{11}(OH)_5]$, and the product was very sensitive to the experimental conditions.^{17,18} Attentions need to be taken to distinguish the slight differences of the synthetic conditions. For example, single crystals of $Ln[B_6O_9(OH)_3]$ and $Ln[B_9O_{13}(OH)_4] \cdot H_2O$ can be obtained when the Ln/B ratios were set to 1/45 and 1/30, together with additional 1 mL and 0.25 mL of H₂O in the starting materials, respectively. 19,20 Here, our synthetic conditions for La_{1-x}Eu_x[B₈O₁₁(OH)₅] ($0 \le x \le 0.135$) (Ln/B = 1/40, 0.5 mL of water, 240 °C) are very close to those for $Ln[B_6O_9(OH)_3]$ and $Ln[B_9O_{13}(OH)_4] \cdot H_2O$. Indeed, if the starting materials were put into the autoclave without a sufficient mixing, the impurity of Eu[B₉O₁₃(OH)₄]•H₂O would appear when x > 0.07. Therefore, we always performed a careful mixing of the starting materials (La₂O₃, Eu₂O₃, H₃BO₃), and the upper limit of the Eu³⁺-doping was extended to 0.135 (without showing any impurity). Because of the size mismatch between La³⁺ and Eu³⁺, we believe the upper limit should not be very high. Anyway, 13.5 atom% is the highest Eu³⁺ concentration we could obtained in current experiments and probably could be increased if the synthetic conditions were further optimized. Note that the very low concentration (~1 atom%) of Eu³⁺ in La[B₈O₁₁(OH)₅] in reference 18 was very likely due to the difficulty in synthesis and also was the reason to the lack of the systematic luminescence investigation. Here we extend this doping to 13.5 atom% and allows the following luminescence study.

The preparation of β -LaB₅O₉ by the thermal calculation of La[B₈O₁₁(OH)₅] has been given in literature, however, this process was reported to be as long as two days at 850 \mathbb{C} .¹⁸ It is a both time-and energy-consuming process. Here we first performed TG-DSC analysis for La_{0.93}Eu_{0.07}[B₈O₁₁(OH)₅]. As shown in Fig. 2a, only one step of weight loss occurs from about 200 to 600 \mathbb{C} due to the gradual dehydration of five hydroxyl groups. The total observed weight-loss of La_{0.93}Eu_{0.07}[B₈O₁₁(OH)₅] is 9.62 wt%, which agrees well with the calculated value 9.23 wt%. From the DSC curve, an obvious endothermic peak presents at 548 \mathbb{C} , related to the dehydration process. Thereafter, another sharp exothermic peak was observed at about 710 \mathbb{C} . Such a peak usually points to a recrystallization process, nevertheless, it needs to be confirmed by powder XRD analysis on the annealed samples at furnace.

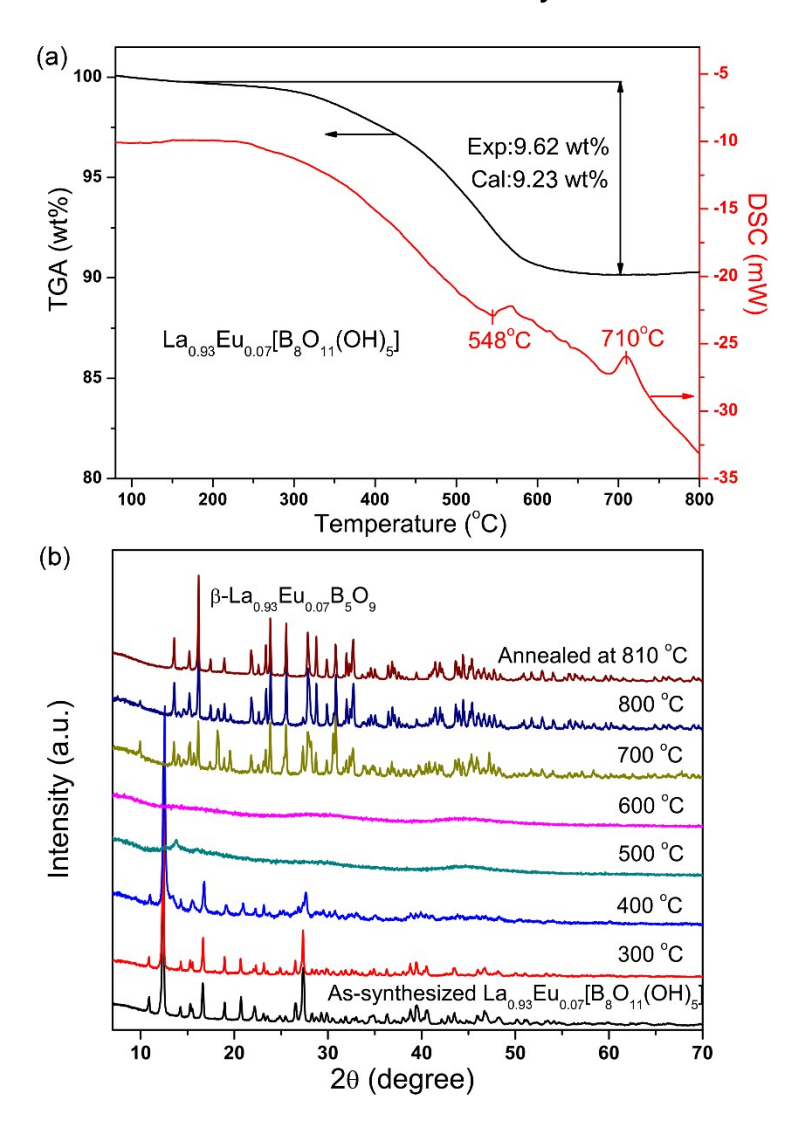


Fig. 2 (a) TG-DSC curves for $La_{0.93}Eu_{0.07}[B_8O_{11}(OH)_5]$ in N_2 atmosphere; (b) powder XRD patterns for $La_{0.93}Eu_{0.07}[B_8O_{11}(OH)_5]$ heated in a muffle furnace at selected temperatures.

As shown in Fig. 2b, La_{0.93}Eu_{0.07}[B₈O₁₁(OH)₅] was heated in a muffle furnace at selected temperatures and checked by powder XRD after cooling down to investigate the thermal behavior. The crystallinity of La_{0.93}Eu_{0.07}[B₈O₁₁(OH)₅] is generally retained until 300 °C. At 400 °C, the diffraction peaks become broad, indicating the crystal structure becomes unstable due to the start of the dehydration process. At 600 °C, it turns to amorphous phase completely, which indicates the dehydration process is complete. Therefore, it is correct that the endothermic peak at 548 °C on the DSC curve corresponds to the continuous dehydration process. After annealing at 700 °C, the amorphous phase undergoes a recrystallization process. As expected, anhydrous pentaborate β-LaB₅O₉ occurs in the product but with some other small impurity peaks (see Fig. 2b). After a further heating at 800 °C, the diffractions of β-

LaB₅O₉ become stronger, while those impurity peaks were finally disappeared after annealed at 810 °C. It becomes clear that those extra peaks belong to an intermediate product, which eventually transform to β-LaB₅O₉ at appreciate high temperature. Readily, the exothermic peak at 710 °C on the DSC curve is attributed to the re-crystallization, and the thermal effect of the intermediate product transforms to β-LaB₅O₉ might be too small or too sluggish to be detected by DSC analysis.

After a careful evaluation of the thermal behavior of La_{0.93}Eu_{0.07}[B₈O₁₁(OH)₅], we prepared β -La_{1-x}Eu_xB₅O₉ by heating La_{1-x}Eu_x[B₈O₁₁(OH)₅] ($0 \le x \le 0.135$) precursors at 810 °C for 10 hours, which is enough to complete the crystallization process and the well-crystalline powder samples were ready for detailed luminescence study.

Phase identification and the successful doping confirmed by XRD

XRD analyses are necessary to verify the phase purity and the success doping of Eu^{3+} , otherwise theses phosphors are not valid for further characterizations. The as-prepared $La_{1-x}Eu_x[B_8O_{11}(OH)_5]$ (0 $\leq x \leq 0.135$) samples are tiny single-crystals, which were finely ground and characterized by powder XRD without observable impurity peaks (see Fig. 3a), moreover, the diffraction peaks slightly shift to higher angles with the increase of x because of the decrease of the ionic radii from La^{3+} to Eu^{3+} . The difference in cell lattice parameters, including a, c and V (summarized in Table S1 in the Electronic Supplementary Information, ESI), can be verified by Le Bail refining of whole XRD patterns using TOPAS (See more details in ESI).²¹ As shown in Fig. 3b, the linear shrinkage of the cell volume along with x is a very strong proof for the successful substitution of La^{3+} by Eu^{3+} in the structure of $La[B_8O_{11}(OH)_5]$.

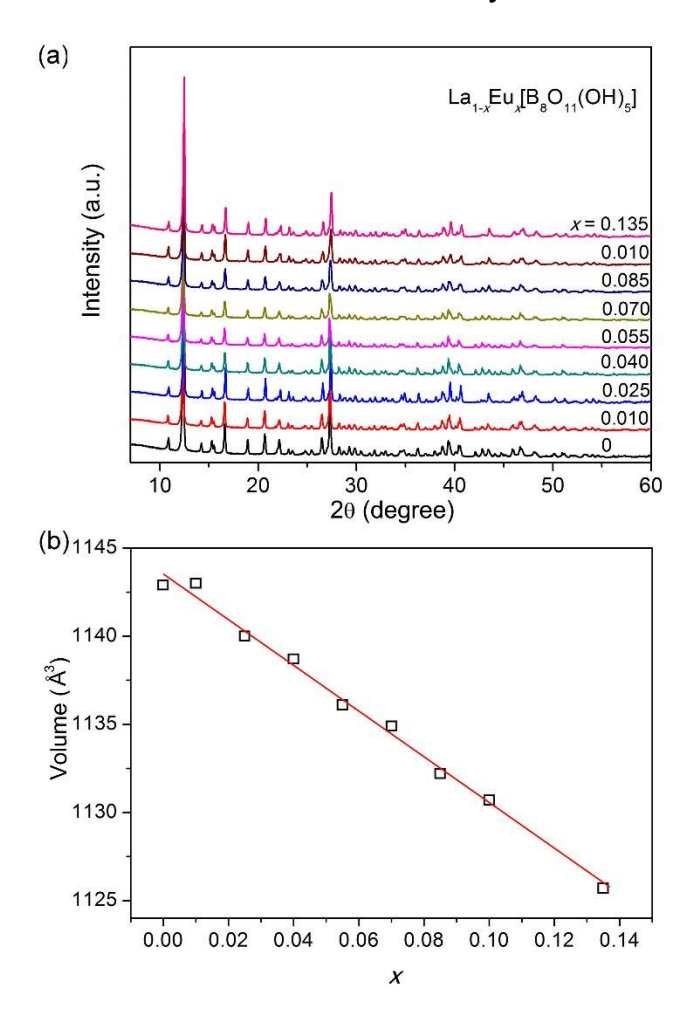


Fig. 3 (a) X-ray diffraction patterns for $La_{1-x}Eu_x[B_8O_{11}(OH)_5]$ ($0 \le x \le 0.135$); (b) the unit cell volumes refined from the Le Bail fitting against the doping content x.

The powder XRD patterns of β -La_{1-x}Eu_xB₅O₉ are shown in Fig. 4a. All diffraction peaks are very sharp indicating all these samples are highly crystallized. By comparison with the simulated XRD pattern for β -LaB₅O₉, it is evident that pure phases of β -La_{1-x}Eu_xB₅O₉ were formed without any impurity peaks. Moreover, the unit cell parameters of these compounds are also obtained by Le Bail fitting, and the refined results are listed in Table S2, ESI. Fig. 4b gives the unit cell volumes against the substitution level (x) for β -La_{1-x}Eu_xB₅O₉. There is a clear shrinking tendency with the doping level, which confirms that Eu³⁺ has been successfully incorporated into the structure of β -LaB₅O₉ without any structural change. All above samples are valid for further luminescence study.

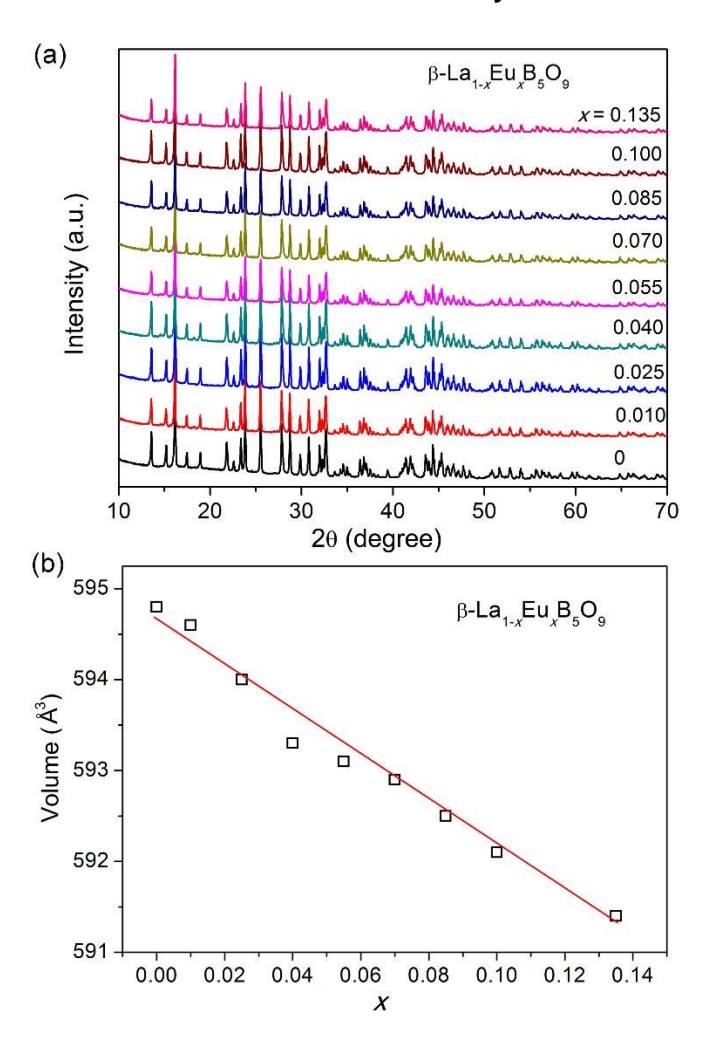


Fig. 4 (a) X-ray diffraction patterns for β -La_{1-x}Eu_xB₅O₉ ($0 \le x \le 0.135$); (b) the unit cell volumes refined from the Le Bail fitting against the doping content x.

Luminescence of hydrous $La_{1-x}Eu_x[B_8O_{11}(OH)_5]$

The excitation spectra of La_{1-x}Eu_x[B₈O₁₁(OH)₅] were measured by monitoring the strongest emission of Eu³⁺ at 622 nm (Fig. 5a). The excitation spectra consist of broad bands in the shorter wavelength region and some sharp peaks in the longer wavelength region. It is clear that the broad absorption bands at about 250-350 nm with maximums at ~275 nm are the typical charge transfer (CT) bands of O²⁻ \rightarrow Eu³⁺.^{22,23} These sharp peaks in the region from 280 nm to 550 nm are due to the 4 f^6 \rightarrow 4 f^6 transitions of Eu³⁺ ions, and the detailed assignments are shown in Fig. 5a. In most Eu³⁺-doped phosphors, the CT absorption is much stronger than the f-f transitions which are parity-forbidden.^{11,22,24} While it is not the case in La_{1-x}Eu_x[B₈O₁₁(OH)₅] (0.010 $\leq x \leq$ 0.135). Similar phenomena were observed

in $Gd_{1-x}Eu_x[B_6O_9(OH)_3]$ and $Sm_{1-x}Eu_x[B_9O_{13}(OH)_4] \cdot H_2O$, where the weak CT absorption might relate to the presence of abundant hydroxyl groups. 19,20 The occurrence of these strong f-f transitions implies the local environment of Eu^{3+} in $La_{1-x}Eu_x[B_8O_{11}(OH)_5]$ is close to noncentrosymmetric, which causes the partial allowance of these f-f transitions. In addition, the intensity of the CT band reaches its maximum when x = 0.085, while the intensities of the f-f excitation peaks of Eu^{3+} increase accordingly with Eu^{3+} concentration. The above characteristics suggest that $La_{1-x}Eu_x[B_8O_{11}(OH)_5]$ may serve as appropriate red-emitting phosphors for WLEDs, which can be efficiently excited by UV-LED chips and show the strongest red emission at 622 nm.

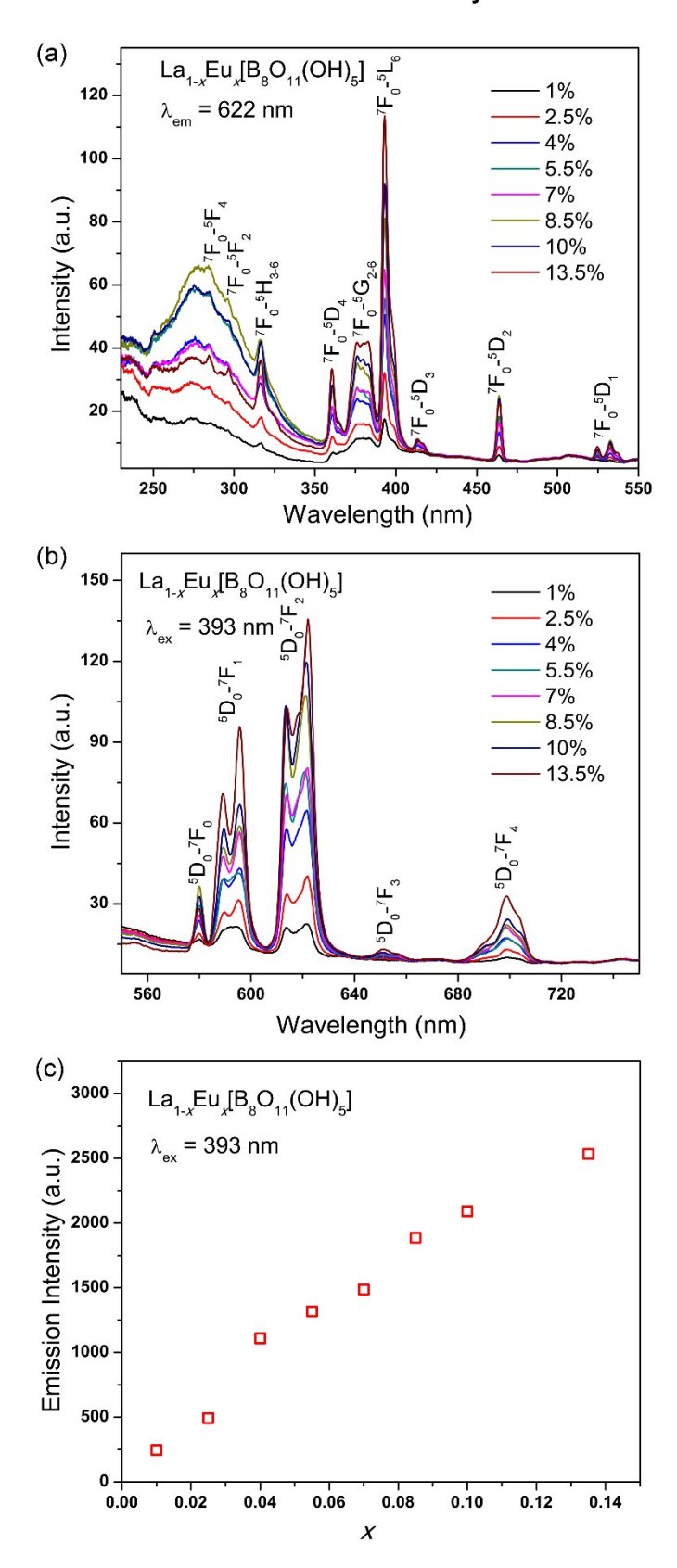


Fig. 5 (a) Excitation and (b) emission spectra for $La_{1-x}Eu_x[B_8O_{11}(OH)_5]$. (c) Dependence of the emission intensity excited at 393 nm against the doping concentration x.

Moreover, it is known that the position of the CT band usually vary according to the change of the local structure of Eu³⁺, which tends to lower wavelength with increasing coordination number and strongly depends on the Ln-O distance as well.^{25,26} As shown in Fig. 5a, the positions of the CT band in the excitation spectra of La_{1-x}Eu_x[B₈O₁₁(OH)₅] (0.010 $\le x \le 0.135$) samples are all located at relatively long wavelength. For instance, these peak wavelength are around 275 nm, while the CT band for other Eu³⁺-phosphors usually locates at ~250 nm.^{27,28} It is reasonable because the La-O bond distances in La[B₈O₁₁(OH)₅] are relative long (with an average value of 2.60 Å).¹⁸ As comparison, the positions of the CT band in Gd_{1-x}Eu_x[B₆O₉(OH)₃] and Sm_{1-x}Eu_x[B₉O₁₃(OH)₄]•H₂O (x = 0.10-1) are all located at relatively shorter wavelengths (~225 and ~232 nm, respectively), ^{19,20} corresponding to relatively shorter Ln-O distances (the average values are 2.42 and 2.50 Å, respectively). ^{17,18} Moreover, the exact peak positions of the CT band in La_{1-x}Eu_x[B₈O₁₁(OH)₅] show a slight red shift from 273 to 277 nm with the gradual increase of Eu³⁺ content (as shown in Fig. 5a), indicating the average Ln-O distance is slightly elongated.

According to the results of excitation spectra, the emission spectra of $La_{1-x}Eu_x[B_8O_{11}(OH)_5]$ were recorded from 550 to 750 nm under the excitation of 393 nm, as shown in Fig. 5b. Five groups of emission peaks at 580, 585-605, 610-635, 645-665, and 680-710 nm were observed, which attribute to the ${}^5D_0 \rightarrow {}^7F_J$ transitions with J = 0-4 of Eu^{3+} ion, respectively.^{22,23} The ${}^5D_0 \rightarrow {}^7F_0$ (at 580 nm) is a single peak, indicating there is only one crystallographic site of Eu^{3+} ion in the structure (Fig. 1a).¹⁸ Moreover, the intensities of the peaks at 614 and 622 nm (${}^5D_0 \rightarrow {}^7F_2$, electric dipole-dipole transition) are all stronger than that of 589 and 595 nm (${}^5D_0 \rightarrow {}^7F_1$, magnetic dipole-dipole transition). As is known, the electrical dipole transition ${}^5D_0 \rightarrow {}^7F_2$ is very sensitive to the local environment around Eu^{3+} , while the magnetic dipole transition ${}^5D_0 \rightarrow {}^7F_1$ is not.²² Therefore, the intensity ratio of red/orange (R/O) = $I({}^5D_0 \rightarrow {}^7F_2)/I({}^5D_0 \rightarrow {}^7F_1)$ is a useful probe of site symmetry for Eu^{3+} . Generally, a lower symmetry of the crystal field around Eu^{3+} leads to a larger R/O.²² For $La_{1-x}Eu_x[B_8O_{11}(OH)_5]$ samples, the R/O are around 2.0, which agrees with the generally noncentrosymmetric coordination environment of La^{3+} in the

structure of La[B₈O₁₁(OH)₅], where La³⁺ is coordinated by 10 oxygen atoms in an irregular environment (see Fig. S3 in ESI). ¹⁸ Moreover, the strongest peak among ${}^5D_0 \rightarrow {}^7F_2$ is located at 622 nm and emissions of ${}^5D_0 \rightarrow {}^7F_4$ around 700 nm were also observable, which are benefit for achieving pure red emission when excited by UV-LED chips. Overall, the emission spectra of the whole series compounds with different Eu³⁺ concentrations generally show the similar characteristic, and the intensities grow with the increase of Eu³⁺ content gradually.

In order to further understand the influence of the Eu³⁺ concentration on the total emission intensity of the samples, Fig. 5c gives the dependence of the total emission intensity on x when excited by 393 nm. A continues and almost linear enhancement was observed, and no quenching or saturation effect was observed. The strongest emission at x = 0.135 is about 10 times of that at x = 0.01. The absence of quenching effect is understandable because Ln^{3+} ions are well separated and therefore diluted by polyborate groups (the nearest Ln-Ln distance is 6.04 Å, as shown in Fig. 1a), ¹⁸ which hampers cross-relaxation or energy transfer between exited and unexcited Eu³⁺ ions.

Luminescence of anhydrous β-La_{1-x}Eu_xB₅O₉

Fig. 6 presents the excitation spectra of β-La_{1-x}Eu_xB₅O₉ (0.010 $\le x \le 0.135$), which were obtained by monitoring the strongest emission at 615 nm. All spectra show similar patterns with a gradual intensity increase along with x. Obviously, the predominant strong absorption band at about 220-340 nm is the typical $O^{2-} \rightarrow Eu^{3+}$ CT absorption; the narrow peaks in the wavelength range of 310-490 nm originate from Eu^{3+} f-f transitions. ^{22,23} The f-f excitations of Eu^{3+} are relatively moderate due to the noncentrosymmetric coordination of Ln^{3+} in β-La_{1-x}Eu_xB₅O₉. ¹⁸ α - and β-LnB₅O₉ are two polymorphs of rare earth pentaborates with different structures. ^{17,18} For α - $Ln_{1-x}Eu_x$ B₅O₉ (Ln = Sm or Gd), the CT bands appear at 220-310 nm with maximums at ~254 nm. ^{19,20} Herein, the maximums of the CT bands in β-La_{1-x}Eu_xB₅O₉ are located at a relatively longer wavelength ~269 nm. As discussed above, such an obvious red-shift implies a longer average Ln-O distances in β-La_{1-x}Eu_xB₅O₉. Indeed, it can be found that the average Ln-O distances for α - and β-LnB₅O₉ are about 2.47 Å (2.29-2.55 Å) and 2.62 Å (2.49-

2.74 Å), respectively, 17,18 which is consistent with the red-shift of CT band from 254 nm (α - Ln_1 - $_x$ Eu $_x$ B $_5$ O $_9$) to 269 nm (β -La $_1$ - $_x$ Eu $_x$ B $_5$ O $_9$). Moreover, in contrast with the parent compounds La $_1$ - $_x$ Eu $_x$ [B $_8$ O $_{11}$ (OH) $_5$], the CT absorptions of β -La $_1$ - $_x$ Eu $_x$ B $_5$ O $_9$ are very strong, and a small blue-shift was found, which might be related to the slight structural contraction after dehydration.

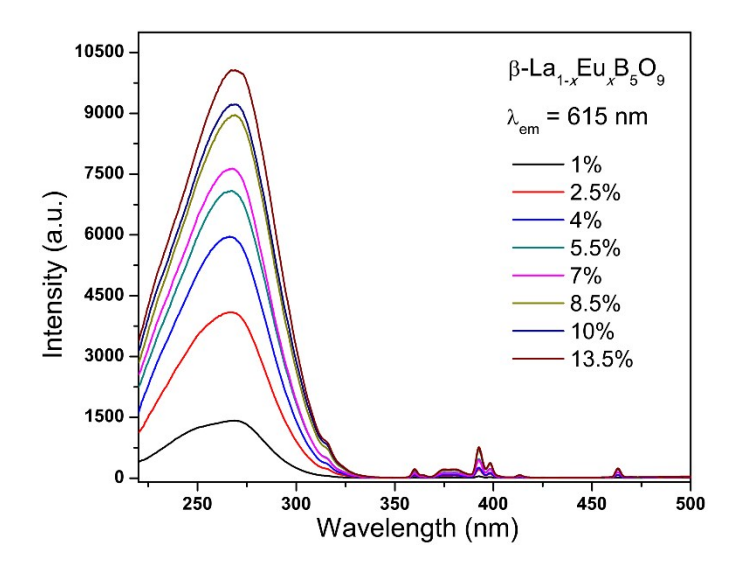


Fig. 6 Excitation spectra for β -La_{1-x}Eu_xB₅O₉ when monitoring the strongest emission at 615 nm.

As shown in Fig. 7a, the emission spectra of β -La_{1-x}Eu_xB₅O₉ show a similar characteristic under the excitation of 269 nm (CT of O²⁻ \rightarrow Eu³⁺). The corresponding emission spectra show emission peaks at 579, 583-604, 608-635, 645-660, and 680-710 nm, which attribute to the typical 5D_0 - 7F_J (J=0-4) transitions of Eu³⁺ ion, respectively.²² In detail, the single peak character of 5D_0 - 7F_0 is consistent with the single crystallographic site of Eu³⁺ ions in the structure (Fig. 1b); 18 the 5D_0 - 7F_1 transitions (583-604 nm) are three separated sharp peaks; the 5D_0 - 7F_2 transitions (608-635 nm) contain at least four peaks (two strong peaks with shoulders), and the total intensity is stronger than that of the 5D_0 - 7F_1 transitions, indicating the local environment around Eu³⁺ is noncentrosymmetric (See Fig. S4 in ESI), which agrees with the crystal structure reported; 18 the 5D_0 - 7F_4 transitions (685-710 nm) contain four main peaks with moderate intensities.

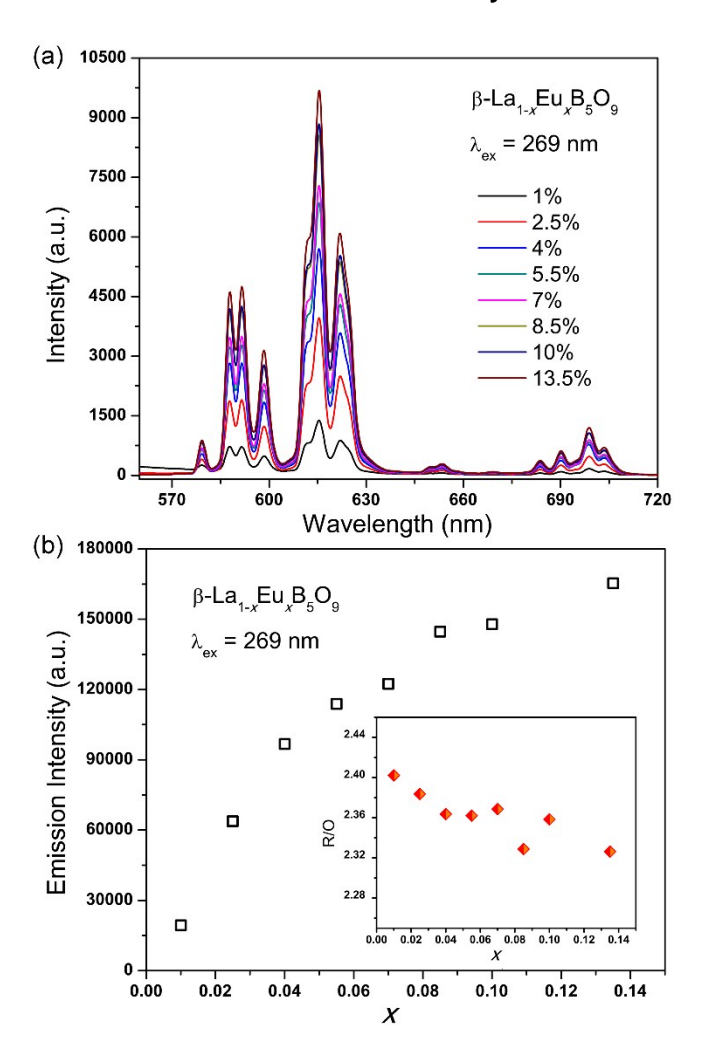


Fig. 7 (a) Emission spectra for β -La_{1-x}Eu_xB₅O₉ when excited by the typical $O^{2-}\rightarrow Eu^{3+}$ CT absorption; (b) dependence of the emission intensity excited at 269 nm against the doping concentration x. The insert shows the red-to-orange ratios.

The influence of Eu³⁺ concentration on the integrated intensity of the total emissions excited by 269 nm (CT of O²⁻ \rightarrow Eu³⁺) are shown in Fig. 7b. It is obvious that the emission increases gradually with x in the whole range. No quenching of the intensities with the increase of Eu³⁺ concentration was observed, which is reasonable due to the large La-La distance in β -LaB₅O₉ (the shortest one is 4.45 Å as shown in Fig. 1b).¹⁸ Moreover, the dependence of the calculated R/O values of β -La_{1-x}Eu_xB₅O₉ on the doping concentration x is shown in the insert of Fig. 7b. The R/O values are around 2.3-2.4 and remain almost unchanged in the whole series, which suggest the relatively small structural change during the substitution. Importantly, the strongest emission peak is located at 615 nm as shown in Fig. 7a, which is benefit for getting pure red emission. When excited by 393 nm (f-f transition of Eu³⁺), the

emission patterns are almost the same with that excited by CT band, but the intensities are weaker (Fig. 8). No concentration quenching was observed as expected. All these results reveal that β -LaB₅O₉ is a good phosphor host for Eu³⁺-doping with intense red emissions but without concentration quenching due to the large La-La distance.

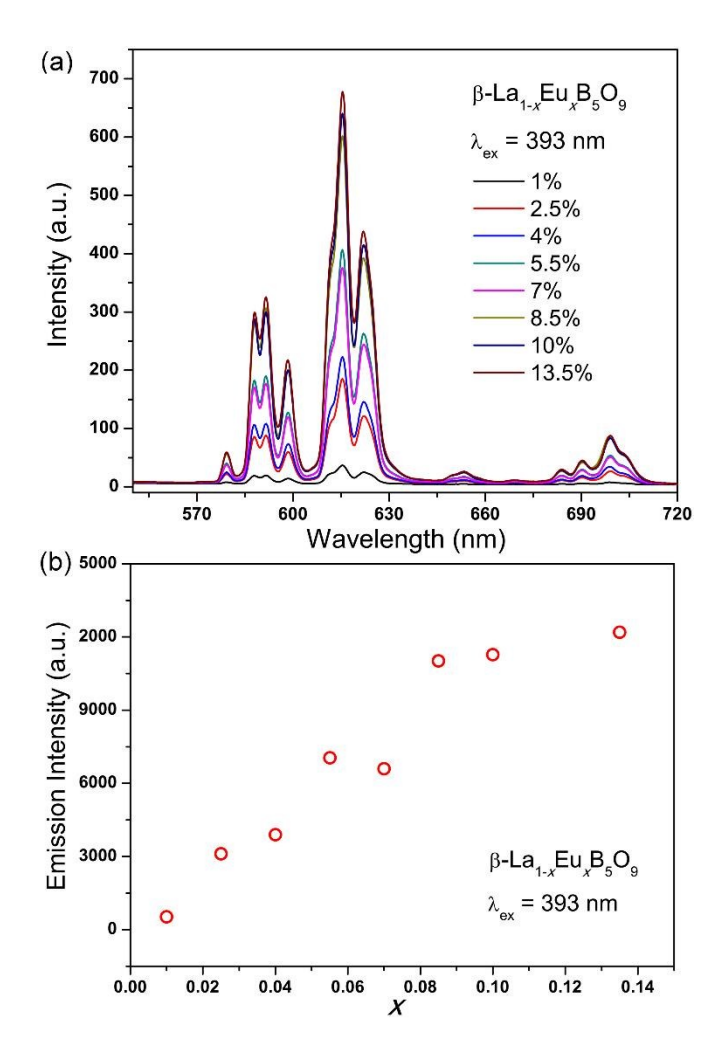


Fig. 8 (a) Emission spectra for β -La_{1-x}Eu_xB₅O₉ when excited by Eu³⁺ f-f absorption at 393 nm; (b) dependence of the emission intensity excited at 393 nm against the doping concentration x.

Luminescence evolution during the thermal transition from $La_{0.93}Eu_{0.07}[B_8O_{11}(OH)_5]$ to β - $La_{0.93}Eu_{0.07}B_5O_9$

As stated above, La_{0.93}Eu_{0.07}[B₈O₁₁(OH)₅] undergoes successive dehydration and recrystallization processes upon heating. On contrary to that only long-range information can be studied by XRD

technique, the luminescence of Eu^{3+} is very sensitive to the local structural information of Eu^{3+} , which therefore is a good medium to gain further information during these thermal processes. Fig. 9 gives the excitation and emission spectra of the annealed products starting from $La_{0.93}Eu_{0.07}[B_8O_{11}(OH)_5]$ at selected temperatures in furnace. The spectra after calcined at 300 $\,^{\circ}$ C are similar to that of as-synthesized sample, indicating the coordination environment of Eu^{3+} remains unchanged. However, the intensities are slightly decreased after 300 $\,^{\circ}$ C calcination, which perhaps originated from the decreasing crystallinity by annealing.

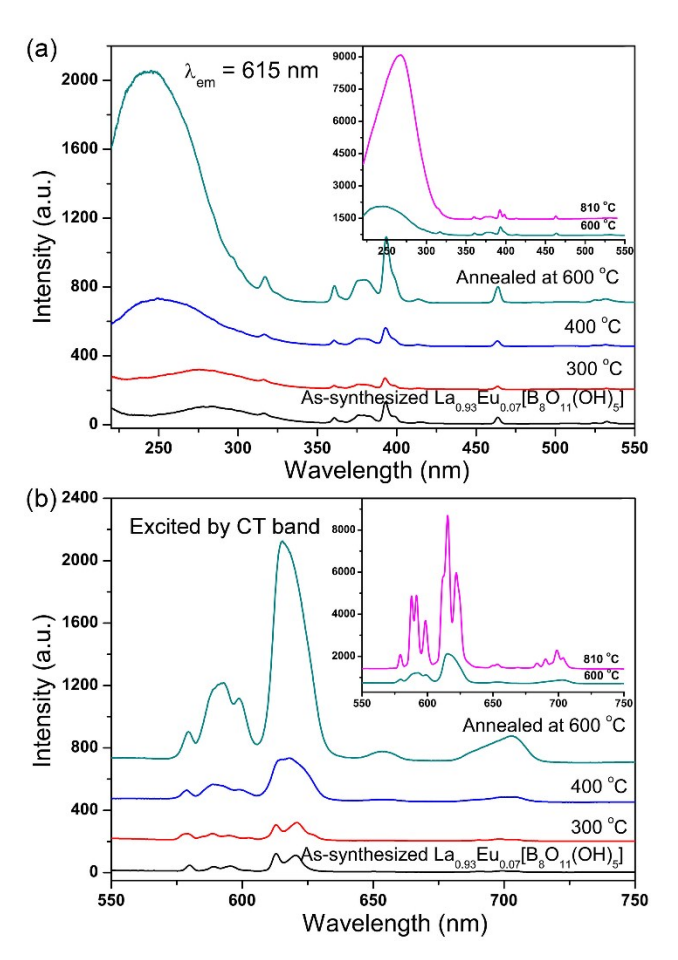


Fig. 9 For the as-synthesized $La_{0.93}Eu_{0.07}[B_8O_{11}(OH)_5]$ and its annealed products at different temperatures: (a) excitation spectra ($\lambda_{em}=615$ nm); (b) emission spectra excited by $O^{2-}\rightarrow Eu^{3+}$ CT absorptions.

At 400 °C, the intensities of both of the CT band and f-f transitions show an obvious increase comparing with that at 300 °C and the CT band shows a blue-shift from 275 nm to 251 nm. As shown

in Fig. 9b, the emission spectrum after annealed at 400 $\,^\circ$ C also shows an obvious intensity enhancement. After annealing at 600 $\,^\circ$ C, both of the excitation and emission spectra show a further and significant intensity increase for more than 5 times. According to the TG-DSC and powder XRD experiments, it is interpreted that the spectra after annealed at 600 $\,^\circ$ C is corresponding to the amorphous phase, and the mixing characteristic of the spectra after annealed at 400 $\,^\circ$ C corresponds to the partial dehydration and some amorphous component forms.

After annealing at 810 °C, the amorphous phase eventually transfers to β -La_{0.93}Eu_{0.07}B₅O₉. The inserts of Figs. 9a and 9b gives the excitation and CT-excited emission spectra of both amorphous phase and β -La_{0.93}Eu_{0.07}B₅O₉. Significant intensity increase and red-shift of the CT band were found by heating at 810 °C. The intensity of *f-f* transitions of Eu³⁺ remains almost unchanged. Meanwhile, similar strong enhancement was also observed for the emission intensity, and a red-shift of the strongest emission peak was found. The profiles of the emission bands become sharper due to the high crystallinity of β -La_{0.93}Eu_{0.07}B₅O₉.

Conclusion

In conclusion, we performed a careful synthesis to prepare La_{1-x}Eu_x[B₈O₁₁(OH)₅] ($0 \le x \le 0.135$) by boric acid flux method, and after evaluating its thermal behavior, an appropriate thermal treatment was applied to prepare anhydrous β -La_{1-x}Eu_xB₅O₉ (810 °C, 10 h), thus allowing the study on their Eu³⁺-luminescence in a relatively wide range of Eu³⁺-concentration. La_{1-x}Eu_x[B₈O₁₁(OH)₅] show the dominant ${}^5D_0 \rightarrow {}^7F_2$ transition, and with the *red/orange* ratio around 2 for all the samples. The comparatively strong f-f transition in the excitation spectra suggests its potential as red-emitting phosphors for white-light emitting diodes, which can be efficiently excited by ultraviolet-light emitting diode chips and show the strongest red emission at 622 nm. On the contrary, β -La_{1-x}Eu_xB₅O₉ show a very intense O²⁻ \rightarrow Eu³⁺ CT absorption, and give strong red emissions with *red/orange* ratios ~2.4. Both the La_{1-x}Eu_x[B₈O₁₁(OH)₅] and β -La_{1-x}Eu_xB₅O₉ show no concentration quenching up to the maximal x = 0.135, which is as-expected due to their large spatial distances between rare earth cations. It is the first

time to study the luminescent performance when $La[B_8O_{11}(OH)_5]$ and β -LaB₅O₉ were used as the hosts. More effects would be needed to further develop their performances.

Acknowledgement

This work was supported by grants from the Natural Science Foundation of China (Grant Nos. 91222106, 21101175, 21171178) and Natural Science Foundation Project of Chongqing (Grant Nos. 2012jjA50012 and 2014jcyjA50036) and the Fundamental Research Funds for the Central Universities (Grant No. CQDXWL-2014-005). We also acknowledge the support from the sharing fund of large-scale equipment of Chongqing University.

Supporting Information Available.

References

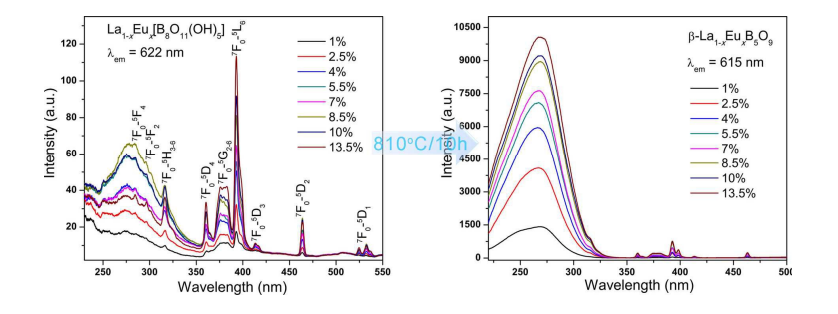
- 1 D. W. Wen, J. J. Feng, J. H. Li, J. X. Shi, M. M. Wu, Q. Su, J. Mater. Chem. C 2015, 3, 2107-2114.
- 2 K. Li, M. M. Shang, D. L. Geng, H. Z. Lian, Y. Zhang, J. Fan, J. Lin, *Inorg. Chem.* 2014, **53**, 6743-6751.
- 3 Q. S. Wu, X. C. Wang, Z. Y. Zhao, C. Wang, Y. Y. Li, A. J. Mao, Y. H. Wang, J. Mater. Chem. C 2014, 2, 7731-7738.
- 4 E. C. Honea, R. J. Beach, S. B. Sutton, J. A. Speth, S. C. Mitchell, J. A. Skidmore, M. A. Emanuel, S. A. Payne, *IEEE Journal of Quantum Electronics* 1997, **33**, 1592-1600.
- 5 B. Saubat, C. Fouassier, P. Hagenmuller and J. C. Bourcet, Mater. Res. Bull. 1981, 16, 193-198.
- 6 K. Machida, G. Adachi, J. Shiokawa, J. Lumin. 1979, 21, 101-110.
- 7 W. Z. Pei, Q. Su, J. Y. Zhang, J. Alloys Compd. 1993, 198, 51-53.
- 8 E. M. Levin, C. R. Robbins, J. L. Waring, J. Am. Ceram. Soc. 1961, 44, 87-91.

- 9 J. H. Lin, M. Z. Su, K. Wurst, E. Schweda, J. Solid State Chem. 1996, 126, 287-291.
- 10 M. Ren, J. H. Lin, Y. Dong, L. Q. Yang, M. Z. Su, L. P. You, *Chem. Mater.* 1999, **11**, 1576-1580.
- 11 J. H. Lin, S. Zhou, L. Q. Yang, G. Q. Yao, M. Z. Su, L. P. You, J. Solid State Chem. 1997, **134**, 158-163.
- 12 J. H. Lin, L. P. You, G. X. Lu, L. Q. Yang, M. Z. Su, J. Mater. Chem. 1998, 8, 1051-1054.
- 13 H. Huppertz and B. von der Eltz, J. Am. Chem. Soc. 2002, 124, 9376-9377.
- 14 J. S. Knyrim, F. Roeβner, S. Jakob, D. Johrendt, I. Kinski, R. Glaum, H. Huppertz, *Angew. Chem. Int. Ed.* 2007, **46**, 9097-9100.
- 15 X. R. Sun, W. L. Gao, T. Yang, R. H. Cong, Dalton Trans. 2015, 44, 2276-2284.
- 16 R. H. Cong, T. Yang, Z. M. Wang, J. L. Sun, F. H. Liao, Y. X. Wang, J. H. Lin, *Inorg. Chem.* 2011,50, 1767-1774.
- 17 L. Y. Li, P. C. Lu, Y. Y. Wang, X. L. Jin, G. B. Li, Y. X. Wang, L. P. You, J. H. Lin, *Chem. Mater.* 2002, **14**, 4963-4968.
- 18 L. Y. Li, X. L. Jin, G. B. Li, Y. X. Wang, F. H. Liao, G. Q. Yao, J. H. Lin, *Chem. Mater.* 2003, **15**, 2253-2260.
- 19 X. F. Yi, R. H. Cong, M. F. Yue, Y. Q. Chai, P. F. Jiang, W. L. Gao, T. Yang, *Dalton Trans.* 2013, **42**, 16318-16327.
- 20 X. F. Yi, R. H. Cong, Z. Y. Zhou, P. F. Jiang, W. L. Gao, T. Yang, New J. Chem. 2014, 38, 122-131.
- 21 TOPAS, V4.1-beta, Bruker AXS, Karlsruhe, Germany, 2004.
- 22 Z. Yang, J. H. Lin, M. Z. Su, L. P. You, Mater. Res. Bull. 2000, 35, 2173-2182.

- 23 Z. J. Liang, F. W. Mo, X. G. Zhang, L. Y. Zhou, P. C. Chen, C. Y. Xu, *Ceram. Int.* 2014, **40**, 7501-7506.
- 24 J. Thakur, D. P. Dutta, H. Bagla, A. K. Tyagi, J. Am. Ceram. Soc. 2012, 95, 696-704.
- 25 G. Blasse, J. Solid State Chem. 1972, 4, 52-54.
- 26 H. E. Hoefdraad, J. Solid State Chem. 1975, 15, 175-177.
- 27 F. W. Tian, C. Fouassier, P. Hagenmuller, Mater. Res. Bull. 1987, 22, 899-909.
- 28 X. X. Li, Y. H. Wang, Z. Chen, J. Alloys Compd. 2008, 453, 392-394.

Graphic Abstract for

Syntheses and luminescence of $La_{1-x}Eu_x[B_8O_{11}(OH)_5]$ and β - $La_{1-x}Eu_xB_5O_9$ ($0 \le x \le 0.135$)



A systematic luminescence study was performed on La_{1-x}Eu_x[B₈O₁₁(OH)₅] and β -La_{1-x}Eu_xB₅O₉ (0 \leq x \leq 0.135), which show bright red emissions.